LPNHE 2006-02

Laboratoire de Physique Nucléaire et de Hautes Énergies
CNRS - IN2P3 - Universités Paris VI et VII

Direct Illumination Led Calibration for Ia Supernovae Photometry

E. Barrelet, C.Juramy

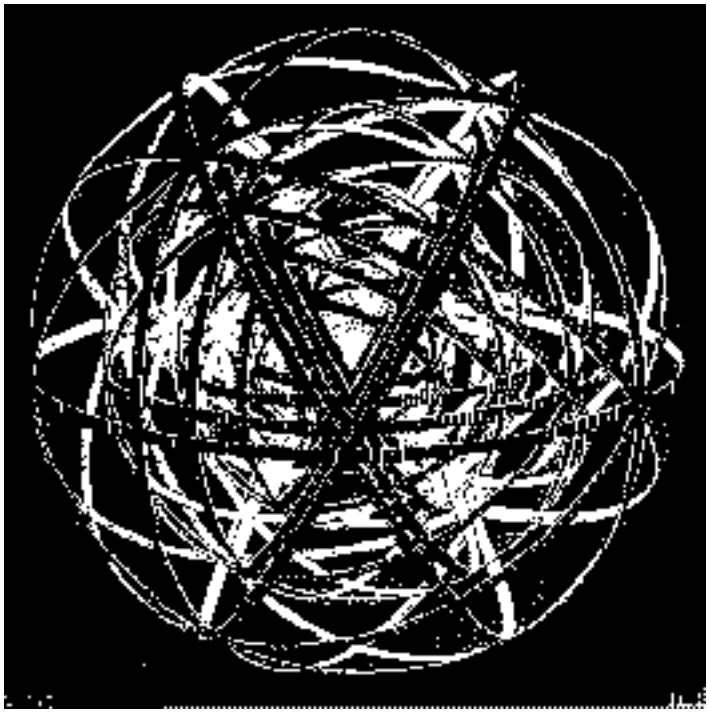

4, Place Jussieu - Tour 33 - Rez-de-Chaussée
75252 Paris Cedex 05
Tél : 33(1) 44 27 63 13 - FAX : 33(1) 44 27 46 38

Abstract

A telescope calibration method for type Ia supernovae photometry is proposed. It is based on the direct illumination of a telescope with a calibrated multi-LED light source. Its description includes traceability of the calibration process and check standard to maintain 0.2% accuracy over years period. Although opto-electronics read-out and control could be built from commercial off-the-shelf components, we report on developments relevant for large systems. Their requirements are tailored on a proposal for the SNLS experiment performed on the Megaprime instrument installed in CFHT for which our R&D is performed. Similar LED systems of larger size are working in high-energy physics optical calorimeters.

1 Introduction

The next generation of cosmology experiments based on type Ia SuperNovae (SN Ia) light curves, either in space or on ground, will have to control the systematic errors affecting the light distance measurements at the 1% RMS level allowed by statistics[1]. This implies the development of new hardware calibration tools and the improvement of SN Ia physical understanding, in addition to the refinement of classical calibration methods based on reference stars. For this reason this paper explores a photometric telescope calibration scheme aiming at a 0.2% accuracy over years periods with a measurement precision better than 1‰. It presents the requirements for a Calibrated Light Emitting Diode (CLED) source providing a direct illumination of the telescope and it will draw an overview of a complete calibration system, including a calibrated Cooled Large Area Photodiode (CLAP) for checking the accuracy. Basic techniques are the same as those used in industrial photometric calibrators. We are using them in our detector test benches as many other groups do. However the operation of an overall telescope calibration system integrating these elements within a large field imager system will be a large enterprise, similar to high-energy physics calorimeters calibration systems [1]. As a first step we shall focus here on generic principles. They still have to be adapted to the various practical applications that we have in mind such as upgrading existing instruments and designing new ground or space instruments. This will be the object of following technical papers beginning with a proposal to equip the SNLS experiment on CFHT/Megacam [2] and the SN Ia option on the Dune proposal [3].

2 Requirements for SN Ia Light Curve Measurement and Calibration

The measurement process characterizing the archetypal SN Ia rolling search experiment is described in [4]. The distance modulus of each SN Ia is extracted from 2 or 3 light curves. Each light curve corresponds to a given wide band filter ($\Delta\lambda/\lambda \approx 22\%$), each point on a light curve corresponds to a given phase ($\Delta\phi \approx 4$ days). Each supernova is a point source with a time-dependent spectral distribution, superposed to a stable galactic extended source. Reference stars which are visible in the field containing the supernova provide one global photometric correction for all atmospheric and instrumental effects. Integral fluxes incoming from a supernova (F_{SN}) and the reference stars (F_*), through a filter F, are estimated using a common aperture definition algorithm.
This process is typically photometric as it reduces the spectral information into “color param-

[1] for an average of 200 SN Ia per Δz=0.1 redshift bin, taking a 15% intrinsic dispersion

eters", e.g. the ratio of B_{SN}/V_{SN} or B_*/V_*. A pure photometric approach is justified when spectra are entirely described by one color parameter expressing their variation around a reference spectrum (Vega). It is the case for Landolt stars and reference stars which are used in SNLS respectively as primary and secondary calibration standards. For these stars the photometric calibration of the instrument consist in determining a few linear coefficients converting the Landolt standard U,B,V,R,I filters into Megacam u',g',r',i',z'. For SN Ia in their rest frame at a given phase the same color parameter approach holds. But a complete spectral model is needed in order to compute the "color corrections" representing the effect of the phase and redshift dependence. For SNLS this spectral model, called "SALT", is described in [5]. This model could be extended to LED or to star calibration. For each light source a rough spectral description should be included in the model, where it enters only as a second order correction to the photometric approximation.

It is clear that a photometric calibration error as a function of λ transforms into an error on the luminosity distance of supernovae as a function of the redshift z. Twenty absolutely calibrated LEDs at $\Delta\lambda / \lambda = 7\%$ allows to check light fluxes with a 0.3% accuracy level for $\Delta z = 7\%$ steps. Besides low and medium resolution sources (star and LED), a high resolution source (laser) as proposed by Stubbs [6] would provide a complementary check on the instrumental model by adding in-situ spectral analysis to factory calibration of filters and CCDs.

3 Calibration Scheme

3.1 principle

In a direct illumination setup, photons propagate between the source and the detector in free space or through a telescope just as starlight does. Consequently the radiation field, besides the emission pattern of the source, depends only on geometrical factors and on the instrument transmission (neglecting multiple reflection effects). When known in one point, the field is known in every other point. This characteristic, combined with those of a LED, namely a point-like, stable, adjustable, bright source with an uniform angular distribution, makes a very attractive photometric calibration scheme. In the telescope calibration setup discussed hereafter, the source emission is restricted by baffling to the angular field of the telescope in order to suppress stray light. The striking characteristic of a LED compared to other sources is its 5-8% FWHM spectral bandwidth. It has positive and negative consequences for our application. On the minus side, one needs around 20 different LEDs to cover the spectral range of a CCD detector. This brings complexity in the control system and in the calibration procedure. On the plus side, the composite LED source offers a spectral granularity finer that the classical UBVRI filter sequence by a factor 3, without the optical and mechanical problems related to the interposition of filters. The spectral distribution of a LED is easy to parametrize and smooth, thus avoiding aliasing problems when testing an optical system having a sharp spectral response such as interferometric filters.

3.2 critical features

Selecting LEDs covering near UV to near IR range is not trivial. Many commercial off-the-shelf LEDs will be rejected because of their plastic dome structure transforming them into an extended source. A point source "flat-top" geometry is preferred (e.g. Agilent P505 green LED shown in Figure 1). In addition a minimal 0.1% LED efficiency[1] is required in order to

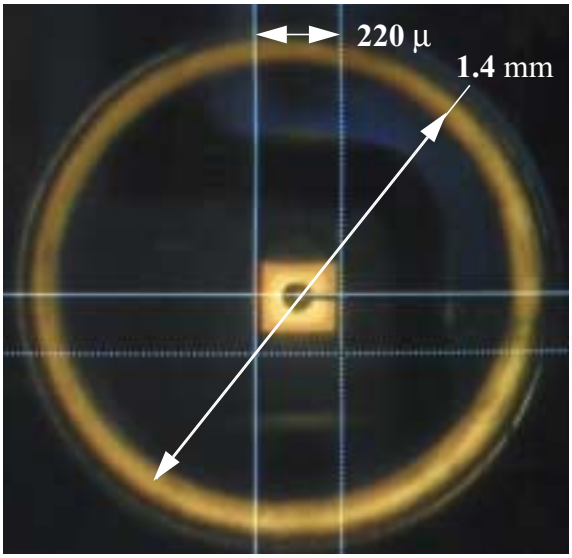

Figure 1 Flat-top square LED (Agilent P505). Its energetic efficiency is 0.1% as computed in Appendix B. Central square (0.2x0.2 mm) is the point source. Outer ring (Ø1.4mm),coming from light diffused on the cylindrical plastic wall, has to be masked.

expose the focal plane detectors to a light flux comparable to the interesting astronomical sources (100 e/pixel/s) for a maximum LED current (50 mA). Photodiodes able to monitor such low fluxes must be cooled and have a large area (1 cm^2) and in order to reach the pico-amp sensitivity. A photometric calibration procedure such as NIST's [7] can be applied to those CLAPs on the optical bench developed for CLED calibration (see Section 3.3) and extended to very low fluxes using the light/distance relationship. Large progress is expected as high efficiency LEDs become commercially available (0.1→10%).

3.3 calibration setup

The setup shown in Figure 2. a) is an optical bench used for the calibration of the CLED source and of the CLAP detector. First it provides the "Integral Radiometric Calibration" (defined in Appendix A) of the CLED source using a calibrated photodiode traceable to NIST[1] mounted on a 3D platform and read with a picoammeter. Secondly the CLAPs, alone or embedded in the focal plane, are calibrated using the CLED source around a one meter distance ("high flux" 1 nA photocurrent). Then the distance between source and detector is increased to d=15 m in order to yield the "low flux" CLAP calibration and eventually to lock the focal plane detector response onto CLAPs.

3.4 telescope setup

Figure 2 b) represents the telescope setup for monitoring a telescope camera, checking calibration accuracy and yielding photometric flat field. The calibrated source is placed in the object space of the telescope, with its axis parallel to the instrument axis. The signal received on the focal plane does not depends on the position of the source, except for the effects of mirror inhomogeneity and angular dependence of secondary optics and focal plane detectors. For a

[1] definitions of LED quantum efficiencies are given in Appendix B
[1] the National Institute of Standards and Technology provides such calibrated detectors

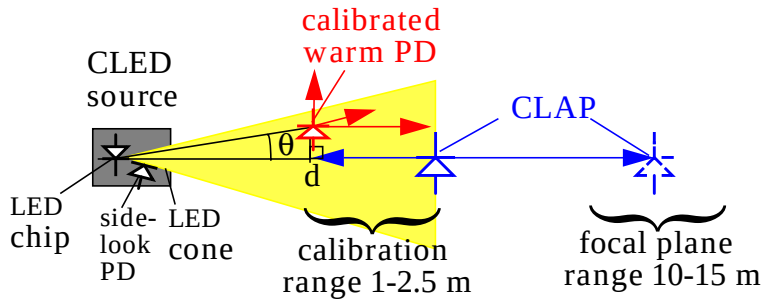

a) calibration setup

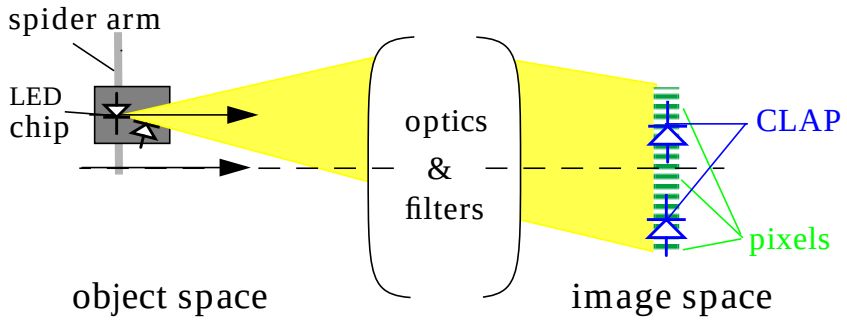

b) telescope setup

Figure 2 a) Setup for the calibration of led light sources (CLED) and cooled large area photodiodes (CLAP). The calibrated PD maps the 3-d radiation field in a θ=3° cone. This yields the 2-d radiant intensity map (W/sr) of the LED, which in turn yields the radiant power received on the CLAP. An extension of the optical bench to 15 m is needed to check the accuracy of CLAP readout at low flux. b) Setup for the calibration of a full telescope (focal plane +optics +filters)

complete factory calibration of the telescope, the light source might scan the entrance pupil of the telescope in order to map the collection efficiency variations across the phase space.
During a SN Ia experiment, the CLED source (fixed for instance to the telescope spider) controls regularly the photometric response of the focal plane detectors and the CLAPs. Technically this provides a “check standard”, as codified in [8]. Practically each “calibration exposure” yields an ideal “flat field” image where the respective response of pixels and CLAPs are proportional to their effective surface. The wavelength resolution of LEDs is ideal to monitor the color dependence of detectors and filters without being bothered by fringing effects. The fluctuations of the focal plane detectors and their electronics can be detected and corrected. Moreover monitoring the response of the CLAPs illuminated by the calibrated light sources controls the long term stability of: a) the telescope transmission, b) the calibrated source itself (using redundancies due to multiple sources and detectors). At the end of the day, the accuracy of the photometric measurements is determined by this long term stability analysis. One find an example of such an analysis in [9] where the collection efficiency of a liquid argon detector varies by 14% in 7 years, while owing to a relevant check standard the accuracy of energy measurement is maintained within 0.3%.

4 Instrument Specifications

These specifications were established for the hardware components developed in view of the calibration of SNLS experiment[10].

4.1 LED Source

This component is a block made of ≈20 identical channels and a common electronic interface. Each channel is composed of a LED, a thermal sink, an optical baffling, a 'side looking photodiode (PD)' for irradiance monitoring, two apertures defining a conical beam (a LED pinhole and an angular diaphragm). With a LED such as seen in Figure 1, core dimensions of this block could be 10 cm in the direction Oz of the optical axis and a 5 cm^2 section xOy perpendicular to it (.25 cm2 per channel). Fabrication is much easier if a larger section is allowed. Positioning precision in the x&y direction should be O(100 µ) in order to assure parallelism of the optical axes. The LED pinhole and angular apertures would be respectively 200x200 µ and Ø=3 mm, assuming a 1° angular aperture surrounded by a 0.1° penumbra region. An extra channel with two pinhole apertures inferior or equal to the LED bright square creates a pencil beam for the alignment of source and telescope axes. The common computer interface contains a temperature sensor, a programmable LED current controller (for addressing LED and setting its illumination level and duration), LED current monitors and irradiance monitors. The irradiance monitors can be coupled to each LED, either by direct illumination, or by quartz fibers[1]. The LED controller generates and reads currents inside closed loops well above noise level. This "current loop" characteristic is favorable for installing analog electronics at a distance from the light source, outside the telescope field of view together with control and readout electronics. Another favorable characteristic is the possibility to cover a large range of radiant power by adjusting or by programming LED currents and to program different exposure duration (electronic and/or mechanical shutter). Table 1 summarize the order of magnitude of the various photodiode currents I_{PD} to measure . The controller system that we have

Location (d)	**LED chip**	**LED cone (2cm)**		**Calibration range (1-2.5m)**		**Focal Plane (15m)**	
detector type		side-lookPD	Q fiber	calibrated PD	CLAP	CLAP	pixel
detector size	200 µ	2 mm	200 µ	5 mm	1 cm	1 cm	15 µ
angular size	1 rad	100 mrad	10 mrad	2-5 mrad	4-10 mrad	0.7 mrad	1 µrad
photon/s	10^{14}	10^{12}	10^{10}	0.4-2.5x10^9	1.6-10x10^9	44x10^6	100
I_{PD} (full scale)	0.4‰x40mA	160 nA	1.6 nA	64-400 pA	0.26-1.6 nA	7 pA	0.016 fA

Table 1 Photon counting rate and photocurrents with LED P505 at 40 mA (efficiency=0.4‰)

described is very similar to several LED pulsing systems which have been built for optical calorimeters in high energy physics experiments. For example in H1-Spacal [11][12] for each calibration event 405 LEDs are illuminating 1600 photomultipliers and 405 photodiodes providing each a measurement precision below 0.1%. It has checked that LED irradiance kept its 0.3% accuracy during 10 years, even without temperature correction [13].

ICI figure pour présenter LED(photo tête de led + scan de la zone d'illumination au picoammeter)

4.2 Cooled Photodiode

The necessity to cool a CLAP in order to suppress dark current is justified by the small photocurrent generated in the focal plane position, as found in Table 1. CLAPs can be mounted in

[1] it is known from HEP calibration systems that tightly held fibers can assure stable optical coupling at 02% for years

the camera's cryostat and share pixels' cooling, or in a small vessel with a Thermo-Electric (T.E.) cooler and a temperature sensor (see Hamamatsu S3477 series). In the former case a Low Current Amplifier (LCA) adapted to the CLAP is the most convenient solution. This is the solution chosen for instance in the NIST amplifier for large area silicon photodiode described in [14]. It can be implemented with a commercial LCA with ultralow input bias current (few fA), in order to monitor photocurrent waveforms of transient LED illumination. The practical problem with this solution is the limited range of a fixed gain LCA. In the latter case, an off-the-shelf picoammeter (e.g. Keithley Model 6485) gives more versatility and performance. In our test bench we have developed a solution cumulating the advantages of both apparatus. It uses a dual gain amplifier [15] connecting the analog output of Keithley 617 Programmable Electrometer to two 16 bits digitizers. This provides a system adding a 0.5 Mhz/ 21 bits waveform digitizer to Keithley's low noise, programmable gain preamplifier with a good electric calibration. On this line we are developping an ASIC integrating an adjustable gain current preamplifier with the same digitizer in order to equip several diodes on the same focal plane [10]. We expect a 1‰ electrical accuracy and a precision <1‰ over a factor 10 on distance, i.e. a factor 100 on current. This corresponds to what is achieved with our current voltage measuring chain described in [16](chap.4).

4.3 Data Processing

This is a real time activity during the whole life of an instrument, producing an enormous data stream, yielding watchdog alerts and providing a feedback on raw data processing. Data taking has to be automatized, if possible with instant data reduction (averaging flat field images etc....). It is not in the scope of this paper, but it is worth remembering that there goes most of the calibration manpower!

5 Conclusion

Progress in LED technology offers high efficiency, point-source packaging and a complete wavelength coverage from near UV to IR. Although it is still difficult to conjugate all these qualities in one LED, it is already possible, with quantum efficiency as low as 0.1%, to illuminate a telescope entrance aperture in order to calibrate photometrically a wide field camera.

We have described a light source covering near-UV to near-IR with 20 LEDs. Its control and monitoring electronics aim at a 0.2% stability and a precision better than 0.1%. It may be calibrated on a classical photometric calibration bench traceable to NIST standard. A low-noise ASIC chain with a 21 bits dynamical range, a precision better than 0.1% and an electric calibration accuracy equal to 0.2% is being adapted to photodiode readout, as an alternative to commercial pico-ammeters. Applied to large cooled photodiodes it may be globally calibrated, using a light distance technique, down to an irradiance level two orders of magnitude lower than allowed by a classical photometric bench. This allows to use photodiodes in a focal plane as a check standard for the overall telescope calibration.

The direct illumination telescope calibration system based on these light source and detector components is well adapted to the requirements of light distance measurements for type Ia supernovae. Absolute photometric calibration of each pixel in a camera at a 0.3% level[1] with a

[1] actually the accuracy of NIST secondary standard might be the limit

7% FWHM spectral “sliding window” is particularly attractive in order to control redshift induced biases. We gave some hints at the complexity of the analysis of the present SN Ia experiments. We are well aware that the system proposed here has to be completed with more classical star calibrators and some spectrophotometric analyses.

Beyond the scope of the SN Ia application, this calibration system has a generic aspect which might interest other science fields. On technical ground, an “absolute photometer” capability allows merging high accuracy data from various experiments, checking high precision modeling of the atmospheric transmission, recalibration of reference stars and improving cosmological distance scale.

Appendix A: Radiometric calibration constants

The “Integral Radiometric Calibration” of a light source assumes that its radiation field is radial. It yields a “radiant intensity” map (W/sr), which transforms into an “irradiance” map *E* (W/m2) in the detector plane when multiplied by a geometrical “inverse square distance” factor. For the geometry of Figure 2-a, this factor is $\cos^3\theta / d^2$. For Figure 2-b, it is the “plate scale” factor ($1/F^2$ where F is the effective focal length of the telescope). The instant response of a photodiode is a photoelectric current *J* characterized by the “Radiant Power Sensitivity” *J*/ Φ (A/W), where $\Phi = E$*A is the radiant power on a detector of surface area A(m^2). This definition supposes that the readout electronics is equivalent to a calibrated ammeter and that the irradiance and the light collection area are known precisely. For imaging detectors the area of a pixel is not known individually with the required accuracy, but it can be assumed on average, supposing a regular paving of the imager. The pixel charge sensing electronics cannot be calibrated individually[1]. Therefore, the imager’s electric sensitivity is expressed in ADC units per exposure time (adu/s) and the calibration constant for each pixel, i.e. the radiant power sensitivity is expressed in (adu/W.s). In order to study deeper the behavior of the imager’s pixels (quantum efficiency, gain, area), a detector model is needed. For instance a model using the same quantum efficiency and same electronic gain for all pixels, adequate for CCDs, would not be applicable to active pixel imagers.

By definition integral radiometric quantities are integrated on the spectral distribution of a specific light source within a wavelength interval $\Delta\lambda$. To each integral quantity corresponds a “spectral” one, for example the “spectral radiant intensity” $I(\lambda)=\delta I/\delta\lambda$ (W/sr/nm). Led spectra being rather narrow ($\Delta\lambda/\lambda^a$ 5-8% FWHM), the factorization of the spectral dependence of the radiation field over phase space is a good approximation.

Appendix B: Quantum Efficiency (Q.E.)

Knowing the average energy of LED photons $\langle h\nu \rangle = e \langle V \rangle$, one can transform the calibration constants of LED and photodiodes into effective quantum efficiencies. First multiply the radiant power sensitivity (A/W) by $\langle V \rangle$ in order to express the PD calibration constant as the average quantum efficiency for Led’s photons α_{PD} (%). Then divide the radiant intensity (W/sr) of a LED by I_{LED}*V in order to express the LED calibration constant as a quantum efficiency α_{LED} (%/sr) for photon emission in the solid angle $\delta\Omega$.

[1] absolute gain is deduced from the photoelectric shot noise (“Poisson” statistics)

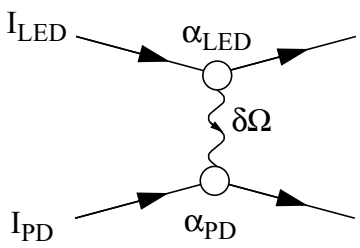

The macroscopic quantity which reflects quantum statistics is the ratio of the currents flowing in a photodiode and in a LED: $I_{PD}/I_{LED} = \alpha_{PD} * \alpha_{LED} * \delta\Omega$ (symbolized by this graph). The probabilities that an electron crossing a LED gap recombines to give a photon and that a photon is converted in a electron-hole pair in the PD are near to 1. Therefore α_{LED} and α_{PD} are essentially the probabilities that a photon goes from LED to air or from air to PD. The fact that $\alpha_{LED} << \alpha_{PD}$ reflects that it is more difficult for light to get from a high to a low refraction index medium than the contrary.

For a numerical application, let us take the specifications of P505 LED (Figure 1):
6.3 mcd/sr= 6.3/683≈9.2 µW/sr at I_{LED}=10mA / $<\lambda>$=0,569 µ (photon energy 2.18 eV).
The number of photons per steradian emitted by an electron in a $\delta\Omega$ solid angle around 0° is:

$$\alpha_{LED} = 9.2(\mu W/sr)/10(mA)/2.18(eV) = 0.042 \quad (\%/sr)$$

The total Q.E. is obtained by integrating the LED emission over solid angle. It corresponds to an effective solid angle Ω_{tot}, equal to 2π, π, $<\pi$, respectively for hemispherical, Lambertian, parabolic emission patterns. Taking $\Omega_{tot}= \pi$, Q.E. is $\alpha_{LED}^{tot} = 0.13\ \%$. The radiometric efficiency (W/W) is almost equal to Q.E. (photon/electron), considering that the mean voltage drop through the LED is about the mean photon energy. The photometric efficiency (lumen/W), usually quoted by industry, is proportional to the radiometric efficiency, the lumen/W constant being 1/683 at λ=0,555 µ. In our example it is 0.89 lm/W, 10 to 50 times smaller than a state-of-the-art efficient LED.

References

(1) ref:HEcaloCAL

(2) General CFHT-Megaprime paper?

(3) Réfrégier et al., astro-ph/0610062

(4) Astier et al., A&A 447 (2006) 31

(5) J.Guy et al., A&A 443 (2005) 781

(6) ref:Stubbs

(7) G.P.Eppeldauer, NIST technical Note 1438 (2001)

(8) NIST/SEMATECH e-Handbook of Statistical Methods, http://www.itl.nist.gov/div898/handbook/index.htm

(9) E.Barrelet et al., Nucl. Instr. and Meth. A 490 (2002) 204

(10) K.Schahmaneche, LPNHE 2006-07

(11) R.D. Appuhn et al., Nucl. Instr. Meth. A426(1999) 518-537

(12) J.Janoth, Thesis, Heidelberg (1996)

(13) J.Ferencei, Private Communication (2006)

(14) G.Eppeldauer and J.E.Hardis, Applied Optics Vol.30, No.22 (1991)

(15) E.Barrelet, C.Juramy, H.Lebbolo, R.Sefri, LPNHE 2004-11

(16) C.Juramy, Thesis (2006)